


Article

A Fluorescent Polyurethane with Covalently Cross-Linked Rhodamine Derivatives

Saiqi Tian ^{1,2,*} , Yinyan Chen ¹, Yifan Zhu ¹ and Haojun Fan ^{2,3}

¹ College of Education, Wenzhou University, Wenzhou 325035, China; 18210411313@stu.wzu.edu.cn (Y.C.); 18210411148@stu.wzu.edu.cn (Y.Z.)

² National Engineering Laboratory for Clean Technology of Leather Manufacture, Sichuan University, Chengdu 610065, China; fanhaojun@scu.edu.cn

³ State Key Laboratory of Polymer Materials Engineering, Sichuan University, Chengdu 610065, China

* Correspondence: tiansaiqi@wzu.edu.cn; Tel.: +86-0577-8668-9665

Received: 1 August 2020; Accepted: 29 August 2020; Published: 1 September 2020



Abstract: Rhodamine derivatives (RDs) with three reactive hydrogens were synthesized and well characterized by Fourier transform infra-red spectroscopy (FTIR), ¹H nuclear magnetic resonance (¹H NMR) and electrospray ionization mass spectra (ESI mass). Then, the obtained RD was covalently cross-linked into polyurethane (PU) matrix through chemical linkages to fabricate a network structure, and the fluorescent properties, mechanical properties, thermal stability, and emulsion particle size were systematically investigated. Results demonstrate that PU-RD maintains initial fluorescent properties and emits desirable yellow fluorescence under ultraviolet irradiation. Moreover, compared with linear PU without fluorescers, PU-RD shows clearly improved mechanical properties and thermal stability, on account of the formed network structures.

Keywords: fluorescent; polyurethane; crosslink; rhodamine

1. Introduction

Recently, significant interest has been directed to the development of fluorescent polymers, because of their intrinsic advantages, including low toxicity, good biocompatibility, long-term stability and better processability [1–3]. In particular, fluorescent polyurethane (PU) is one of the most desirable polymers, owing to its outstanding combination of unusual features, such as excellent mechanical strength, good abrasion resistance, and high elasticity [4–7]. These facilities make the materials useful for technological applications in a very broad range of fields, such as coating materials, textiles, paper making, organic light emitting diodes (LEDs), and fluorescent probes. For example, Lian and coworkers [8] designed and prepared a fluorescent polyurethane nanocomposite via one-pot in situ synthesis methods. This the fluorescence of composites can be changed with various carbon precursors with different structures, showing wide potential application for flexible solid-state lighting and displays.

A fluorescent PU is mostly made of a mixture of fluorescers and polymer. However, physically doping fluorescers into PU matrices inevitably leads to some shortcomings, including poor mechanical properties and incompatibility with the matrix, attributed to weak interaction between fluorescers and PU [9]. Generally, PU structure is determined by raw materials, hard and soft segment, molecular weight, polydispersity, and cross-linking ability. It can be easily designed by changing the types and quantities of socyanate, polyol, surfactants, catalysts, fillers, and cross-linking agents during the manufacture process or via advanced characterization techniques, so as to meet the desired performance [10–12]. Thus, attention has been drawn to the chemical attachment of small molecular fluorescers into polyurethane backbones.

As commonly recommended coating materials, PU is supposed to exhibit good mechanical properties and ideal thermal stability [13–15]. As mentioned before, the final properties have the possibility to be tailored by changing the composition. In addition, PU properties highly depend on the chemical cross-linking of the polymer chains. It is regarded that moderate cross-linking can positively influence these performances [16,17]. Previous research has proved that the thermal stability of cross-linked polyurethanes is higher than that of the linear one [18,19]. Network structures also result in improvement of mechanical properties [20,21]. Some works have been devoted to the influence of crosslinker on properties of PU. For example, Arévalo-Alquichire et al. [22] synthesized a PU using pentaerythritol as a crosslinker. Results indicated that the largest concentration of cross-linkers produced more distributed segment segregation and higher thermal stability. Cross-linking process in PU could be carried out through various methods, wherein low-molecular-weight compounds with more than two reactive hydrogens were used as cross-linkers, such as trimethylolpropane (TMP) and triethanolamine (TEA) [23–25]. Moreover, rhodamine chromophores have advantages of long wavelengths of excitation (greater than 550 nm) and emission (590 nm), good photostability, and high fluorescent quantum yields. They are widely used fluorescent micromolecules [26]. However, the report of using rhodamine derivatives as polyurethane cross-linkers is still very scarce. Guided by these previous findings, we designed and synthesized rhodamine derivatives (RD) with three reactive hydrogens, which are ideal cross-linkers for PU. Subsequently, fluorescent polyurethanes (PU-RDs) were prepared by being covalently cross-linked by RD. The fluorescent properties, mechanical properties, thermal stability, and emulsion particle size of PU-RDs were fully investigated. Our results verify that PU-RDs exhibit very promising and unique properties. PU-RDs maintain appealing fluorescent properties after polymerization with RD, and emit yellow fluorescence under a ultra-violet (UV) lamp. As result of network structures, PU-RDs present higher mechanical properties and thermal stability than linear PU. The easy-to-obtain materials, facile preparation, good mechanical properties, and thermal stability make it suitable for potential practical applications.

2. Experiment

2.1. Materials

1,4-butanediol (BDO), 2,2-bis (hydroxymethyl) propionic acid (DMPA), triethylamine (TEA) were purchased from Micxy Chemical Co., Ltd. (Chengdu, China). Isophorone diisocyanate (IPDI), rhodamine 6G, 2-aminoethano, acetonitrile, and acetone were supplied by Aladdin Industrial Corporation (Shanghai, China). Poly(propylene glycol) with molecular weights of 2000 (PPG220) and polytetrahydrofuran glycol with molecular weights of 1000 (PTMG210) were sourced from Dow Chemical Company (Midland, MI, USA) and dried at 120 °C under high vacuum (0.5 mmHg) for 12 h before use. Bismuth neodecanoate was provided by Deyin Chemical Co. Ltd. (Shanghai, China).

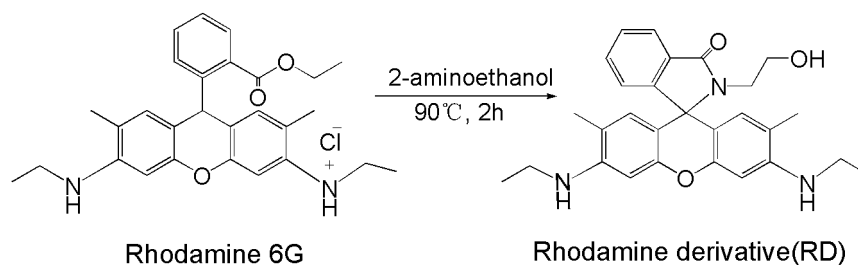
2.2. Synthesis of Rhodamine Derivative (RD)

Rhodamine 6G (5 g, 10.4 mmol) was dissolved in 80 mL of acetonitrile. Thereafter, 2-aminoethanol (1.85 mL, 31.3 mmol) was added to the solution. The reaction was stirred under reflux at 90 °C for 2 h (See Scheme 1). After that, the mixture was cooled to room temperature. The solid was filtered and washed with water three times, and dried under vacuum. Yield: 93%.

2.3. Synthesis of Fluorescent Waterborne Polyurethane (PU-RD)

IPDI, PPG220, PTMG210, and BDO (molar ratio IPDI: PPG220: PTMG210: BDO = 6:6:1:1.6) were poured into the four-necked separable reaction flask equipped with a mechanical stirrer, thermometer, nitrogen inlet, and condenser with a drying tube. The mixture was heated to 80 °C with a drop of bismuth neodecanoate (0.05 wt. %) as a catalyst, and the reaction was carried out for 2–3 h. Afterwards, the intermediate was chain extended by adding DMPA (molar ratio of IPDI: DMPA = 6:1.1) at that temperature for another 2 h to form a liner prepolymer. During the pre-polymerization, a suitable

amount of acetone was added to dilute the viscosity of the reaction system. Successively, RD was added and the pre-polymerization was carried out at 80 °C under N₂ atmosphere for a duration of 2 h. After that, the system was cooled to 50 °C. As a neutralization agent, TEA (molar ratio TEA: DMPA = 1.1:1) was then added to react with the carboxylic group. Ultimately, the resultant mixture was dispersed by appropriate deionized water with vigorous stirring conditions for 1.5 h. The final PU-RD was obtained, and the solid content of the emulsion was approximately 30%. Samples here are abbreviated as PU-RD-x, and the corresponding RD weight concentrations of PU-RD-1, PU-RD-2, PU-RD-3, and PU-RD-4 are 0.5%, 1.0%, 1.5%, and 2.0%, respectively.



Scheme 1. Synthesis of RD.

As a control, linear polyurethane (PU) was synthesized using the same procedure without the presence of RD.

2.4. Measurements

Fourier transform infra-red (FTIR) spectra were obtained with a Nicolet IS10 FTIR spectrometer (ThermoFisher Scientific, Waltham, MA, USA) in the range from 400 to 4000 cm⁻¹ with 32 scans at 2 cm⁻¹ resolution. ¹H nuclear magnetic resonance (¹H NMR) spectra were acquired on a AV400 NMR (400 MHz; Bruker, Ettlingen, Germany) spectrometer operating in the Fourier transform mode at 30 °C with deuterated dimethyl sulfoxide (DMSO-d₆) as the solvent and tetramethylsilane as the internal reference. Electrospray ionization (ESI) mass spectra were obtained on a Finnigan LCQ Advantage ion trap mass spectrometer (ThermoFisher Corporation). The fluorescent emission properties were measured at room temperature using a spectrophotometer (Fsp920, Edinburgh Instruments, Livingston, UK) and the slit was 1 nm in width. The DMA measurements were conducted in the three-point mode with DMA Q800. Tensile tests (tensile strength and elongation at break) were carried out on the samples with a universal material testing machine (model tensiTECH) supplied by Tech-Pro Inc. (Woodstock, NY, USA) at room temperature. The samples were cut into dumb-bell shapes with a thickness of around 1.0 mm and the crosshead speed was set at 10 mm min⁻¹. For each data point, five samples were tested to obtain an average value. Thermogravimetric analysis (TGA) was performed with a TG-209 F1 thermal analyzer (Netzsch, Germany) at a scanning rate of 10 °C min⁻¹ under a nitrogen flow rate of 60 mL min⁻¹. Particle sizes were obtained by laser particle size analyzer (Mastersizer 3000E).

3. Results and Discussion

3.1. Structure Characterization

The chemical structure of RD was analyzed by FTIR spectroscopy, ¹H NMR, and ESI mass. Figure 1 presents FTIR spectra of rhodamine 6G and RD. After modified by 2-aminoethanol, the FTIR peaks at 2363 cm⁻¹ and 2342 cm⁻¹, which are assigned to NH⁺ in rhodamine 6G, disappear. Moreover, the peak of -C=O distinctly blue-shifts from 1716 cm⁻¹ to 1682 cm⁻¹, on account of the transformation from ester linkage (-COOC-) [27] to amido linkage (-CO-N-) [28]. Figure 2 displays digital images of rhodamine 6G and RD in daylight. The color of powders is obviously changed after reaction. The ¹H NMR spectrum of RD is depicted in Figure 3, and we can find the corresponding peaks: δ 7.94 (m, 1H),

7.48 (m, 2H), 6.97 (m, 1H), 6.22 (s, 2H), 6.16 (s, 2H), 3.32 (s, 2H), 3.14 (m, 2H), 2.50 (s, 4H), 1.23 (m, 6H). Furthermore, the mass of RD ($C_{28}H_{32}O_3N_3$) is calculated to be 458.58. As presented in Figure 4, the ESI mass measured mass is 458.24. All these results indicate the successful synthesis of RD.

PU-RD-3 was chosen as a representative example to confirm the structure of PU-RD by FT-IR spectrometry, as shown in Figure 5. We can find the typical peaks of PU, including those at 3334 cm^{-1} (N–H stretching), 2970 and 2931 cm^{-1} ($-\text{CH}_3$ and $-\text{CH}_2-$ stretching), 1705 cm^{-1} (C=O group in urethane) and 1108 cm^{-1} (C–O–C stretching) [29]. The characteristic absorption peak of semicarbazide formed from the reaction of $-\text{NH}-$ in RD and $-\text{NCO}$ in IPDI is observed at 1673 cm^{-1} in the spectrum of PU-RD, indicating that RD has been successfully implanted into the polyurethane main chains [30].

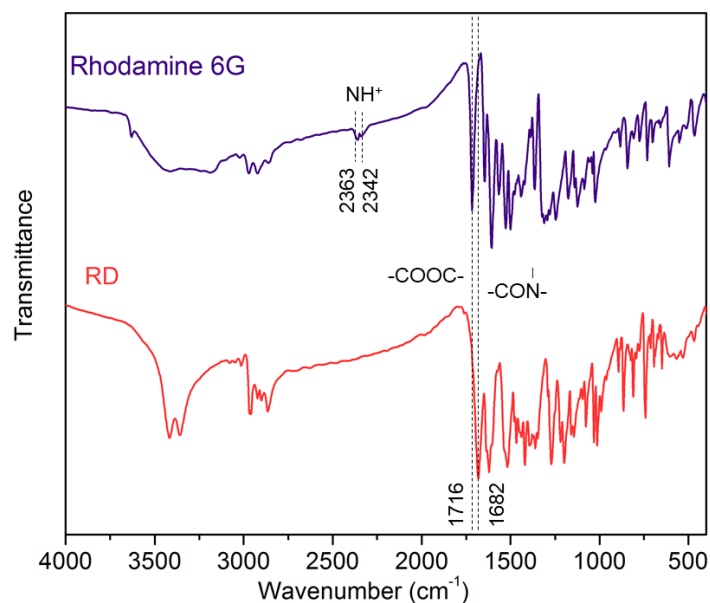


Figure 1. FTIR spectra of Rhodamine 6G and RD.



Rhodamine 6G

RD

Figure 2. Digital images of Rhodamine 6G and RD.

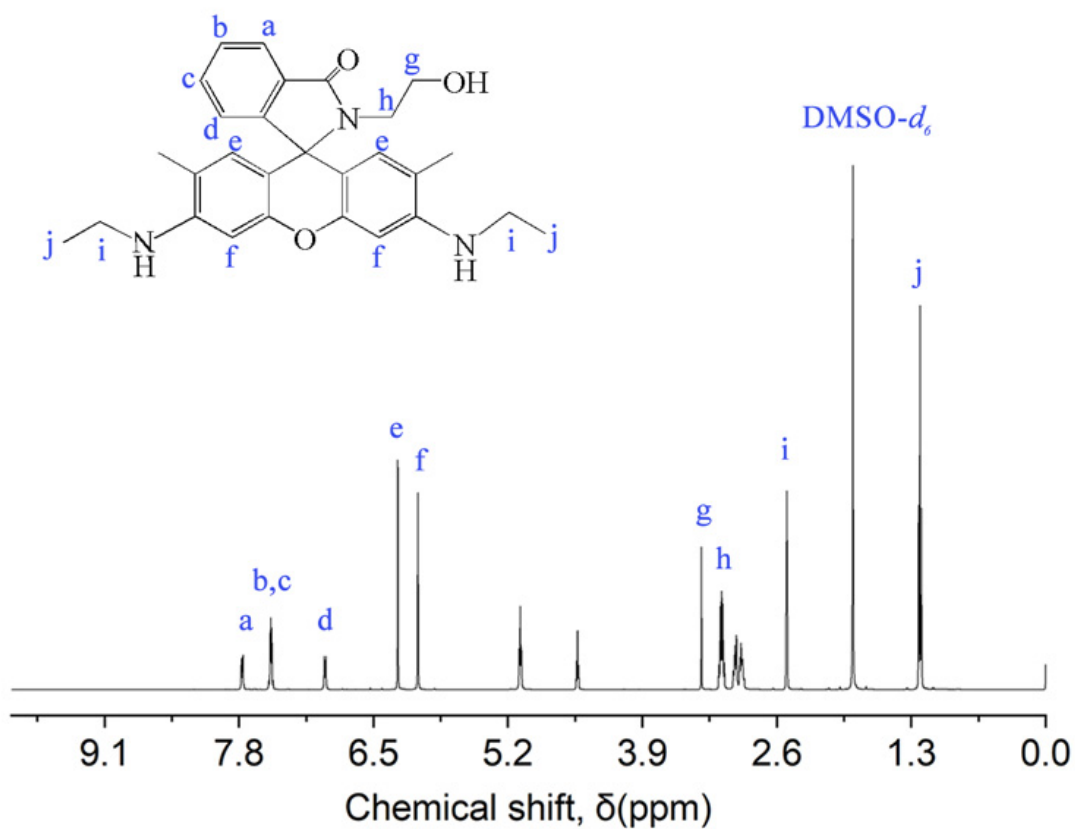


Figure 3. ¹H NMR spectrum of RD.

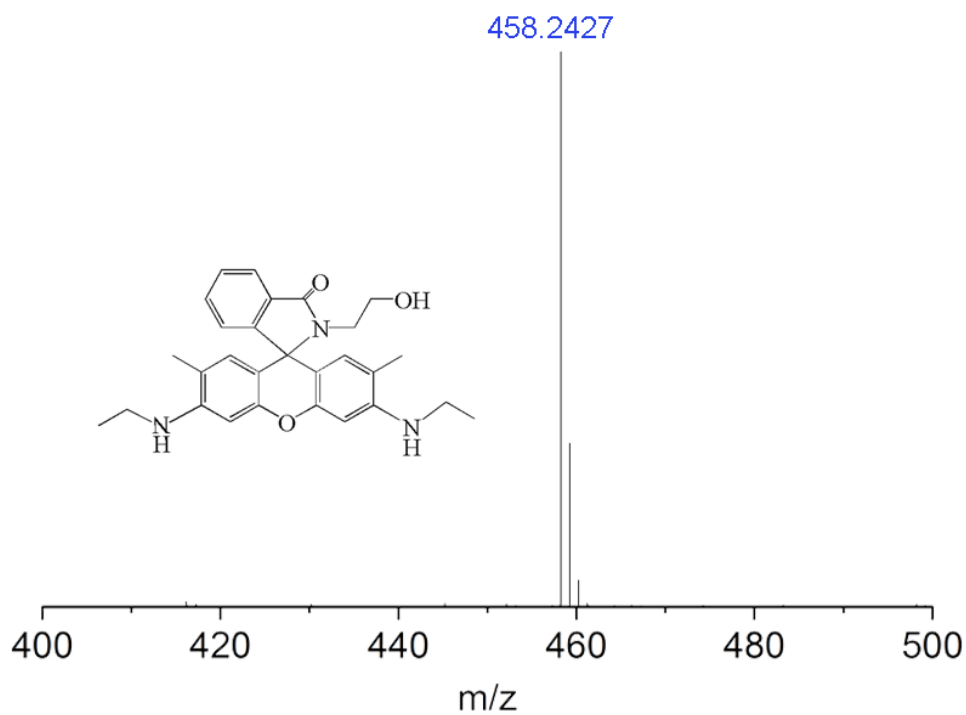


Figure 4. ESI mass spectrum of RD.

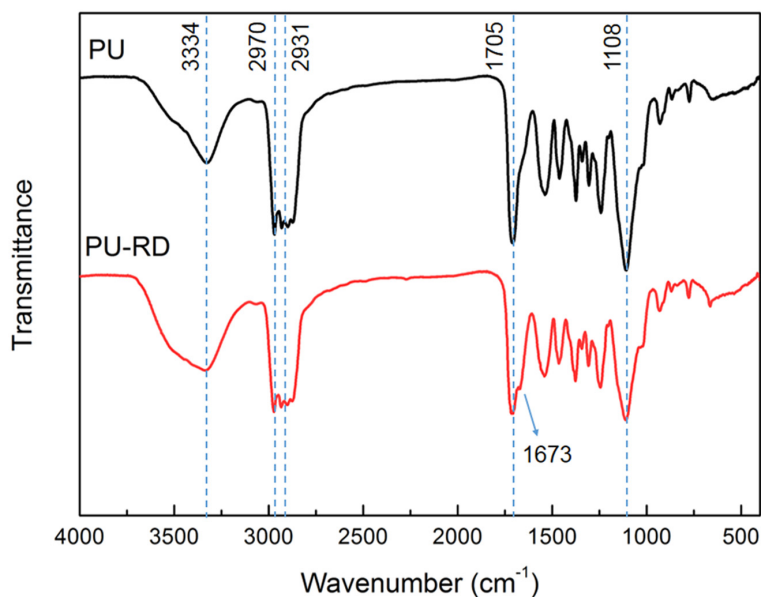


Figure 5. FTIR spectra of PU and PU-RD.

3.2. Fluorescent Properties

To evaluate the fluorescent properties of PU-RDs, their fluorescence spectra were acquired. The fluorescence spectra of RD, PU, and PU-RDs, assessed by the wavelengths 365 nm at 25 °C, are displayed in Figure 6. It can be seen that PU without RD unit shows no emission peaks, while RD and PU-RDs show similar emission shape and the maximum emission wavelength. This demonstrates that the PU-RDs still maintain appealing fluorescence after polymerization. After being attached into PU networks, the local environment around the RD fluorophores is changed [31]. Consequently, compared to the spectrum of RD, the maximum peaks of PU-RDs shift from 560 nm to 556 nm and show a hypochromatic shift. In addition, the maximum intensity of PU-RDs gradually increases as the content of RD increases.

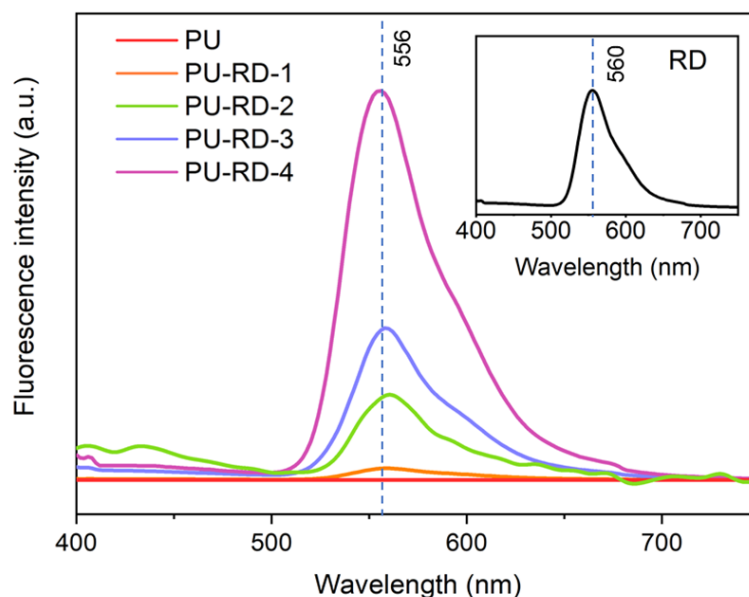


Figure 6. Fluorescent emission spectra of PU and PU-RDs. The inset is fluorescent emission spectrum of RD.

Figure 7 depicts images of PU and PU-RDs films taken both in daylight and in darkness under 365nm ultraviolet irradiation. We can see that PU-RDs present red in daylight. In darkness, PU without RD shows no light emission. It is quite clear that PU-RDs emit yellow fluorescence under a 365 UV lamp.

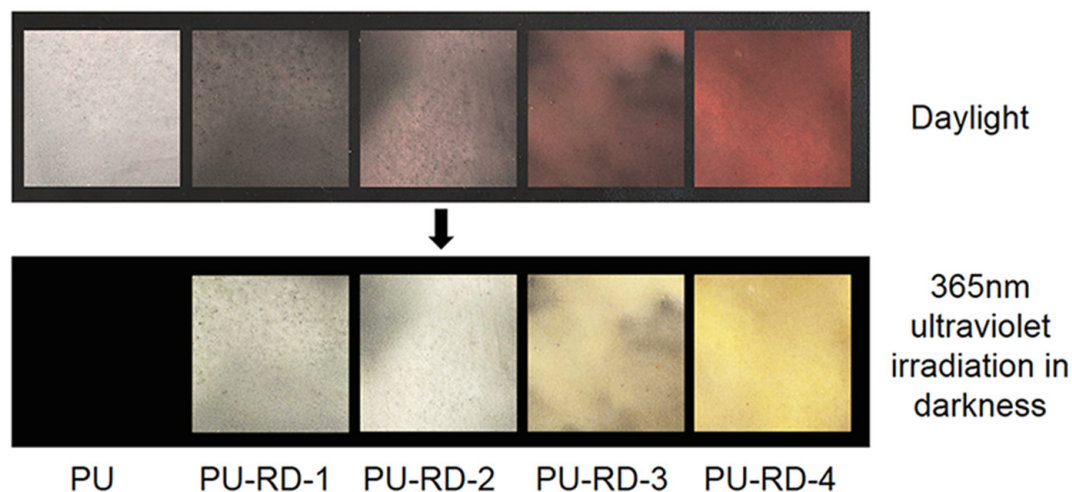


Figure 7. Digital images of PU and PU-RDs taken in daylight and under 365nm UV irradiation in darkness.

3.3. Mechanical Properties

Tensile tests and dynamic thermomechanical analysis (DMA) were performed to measure the mechanical properties of PU and PU-RDs, and the results are summarized in Table 1. Figure 8 displays stress–strain curves of PU and PU-RDs. As the content of RD increases, the tensile strength enhances and the elongation at break weakens, owing to the cross-linking of polyurethane by $-OH$ and two $-NH-$ of RD. The dissipation factor ($\tan \delta$) curves as a function of temperature for the PU and PU-RDs are given in Figure 9, where the peak of $\tan \delta$ is defined as the glass-transition temperature (T_g) [32,33]. The higher cross-linking density also restricts polymer-chain mobility, leading to the increase of glass-transition temperature [34,35].

Table 1. Mechanical Properties of PU and MFPU; Shown Are Tensile strength, Elongation at Break and Glass-Transition Temperature (T_g).

	Tensile Strength (MPa)	Elongation at Break (%)	$T_g/^\circ\text{C}$
PU	10.0	840.0	−43.9
PU-RD-1	10.5	763.9	−41.3
PU-RD-2	11.0	711.8	−39.6
PU-RD-3	12.3	632.2	−36.2
PU-RD-4	14.5	544.1	−33.4

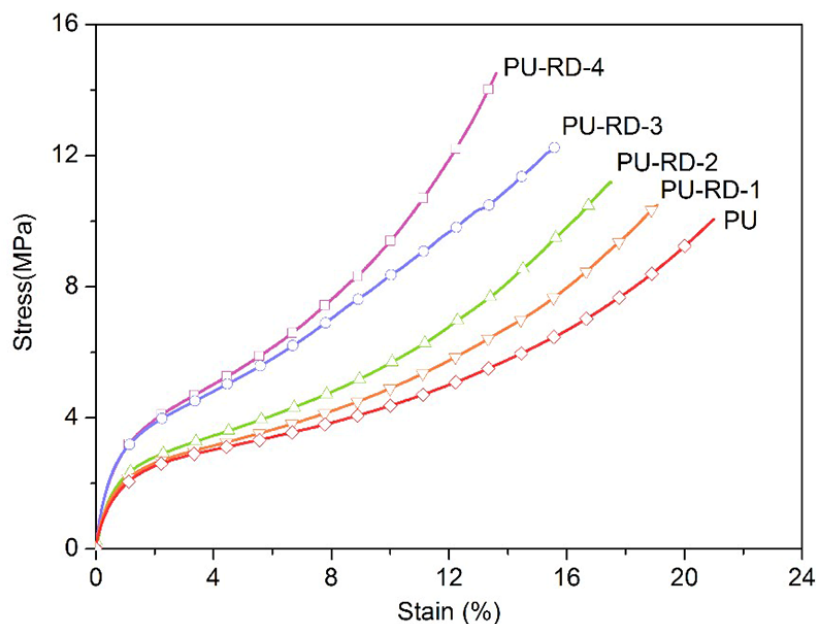


Figure 8. Stress–strain curves of PU and PU-RDs.

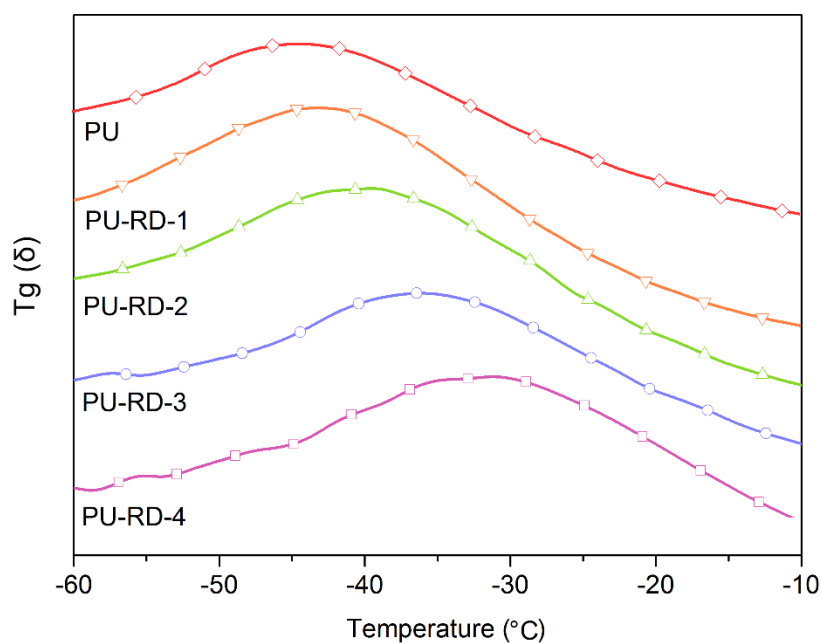


Figure 9. DMA curves of PU and PU-RDs.

3.4. Thermal Stability

The thermal stability of polyurethanes is a significant parameter for their application as a coating material. PU-RD-3 was chosen as a representative example to study the thermal stability. TGA and differential thermogravimetric (DTG) curves of PU and PU-RD-3 are given in Figure 10a. The corresponding data are briefly summarized in Table 2. In general, the TGA curves for the two samples are similar. PU-RD-3 displays slightly higher thermal stability. There is a typical three-step decomposition process. The first step under 300 °C is ascribed to the evaporation of acetone and water [36]. The initial weight loss (temperature taken at the 5 wt. % of weight loss, $T_{5\%}$) for PU and PU-RD-3 appears at 279.2 and 281.9 °C, respectively. The second step corresponds to the decomposition of hard segments i.e., urethane groups [37]. T_{max1} of PU and PU-RD-3 is at 330.4 and

346.6 °C, respectively. PU-RD-3 is cross-linked by RD, and the network structures present higher thermotolerance [35]. Moreover, the RD, composed of three benzene rings, is supposed to exhibit good thermal stability and is difficult to decompose with increasing temperature [38,39]. Both the network structures and the attachment of benzene units as hard segments result in a higher $T_{\max 1}$. The third step is related to soft segments (ether or ester bond) [40]. The weight-loss curves are similar during this step. Therefore, PU-RD has good stability in the storage and application.

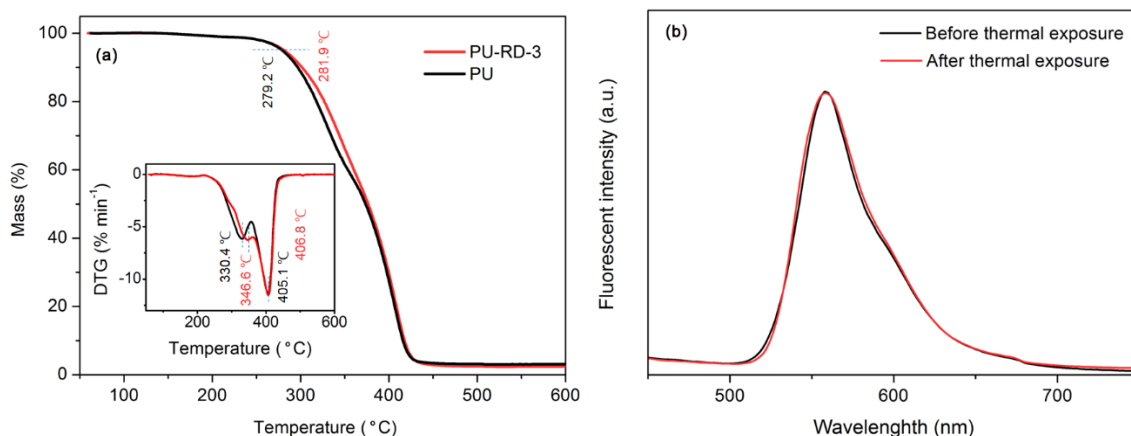


Figure 10. (a) Thermogravimetric and curves and DTG of PU and PU-RD-3; (b) Fluorescent emission spectra of PU-RD before and after thermal exposure.

Table 2. TGA and DTG results for PU and PU-RD-3.

	$T_{5\%}^a/^\circ\text{C}$	$T_{\max 1}^b/^\circ\text{C}$	$T_{\max 2}^c/^\circ\text{C}$
PU	279.2	330.4	405.1
PU-RD -3	281.9	346.6	406.8

^a Temperature at 5 wt. % weight loss; ^b Temperature at the max rate of step 2 weight loss; ^c Temperature at the max rate of step 3 weight loss.

The fluorescent properties are also expected to be stable after thermal exposure. PU-RD-3 was kept at 100 °C for 24 h in an oven. Then, the fluorescent emission spectrum was obtained. From the fluorescent emission spectra in Figure 10b, we can see that the maximum peak and shape of PU-RD are almost the same before and after thermal exposure, demonstrating desirable stability.

3.5. Emulsion Particle Size Analysis

Figure 11 depicts the particle size distribution of PU and PU-RDs emulsions, respectively. The detailed data for average size and particle dispersion index are summarized in Table 3. The average size of PU is 48.20 nm. Regarding PU-RD-4, it is measured to be 78.82 nm. The cross-linkers are copolymerized with PU chains, forming network structures. Therefore, the molecular chains get stiffer, leading to poorer hydrophilicity. This is unfavorable for emulsification and dispersion [41]. Consequently, the average sizes gradually decrease as the content of RD increases. Furthermore, with the incorporation of RD, the particle dispersion index gets narrower. With more network structure formed during the polymerization, more molecules are intertwined around major structures, as described in Figure 12.

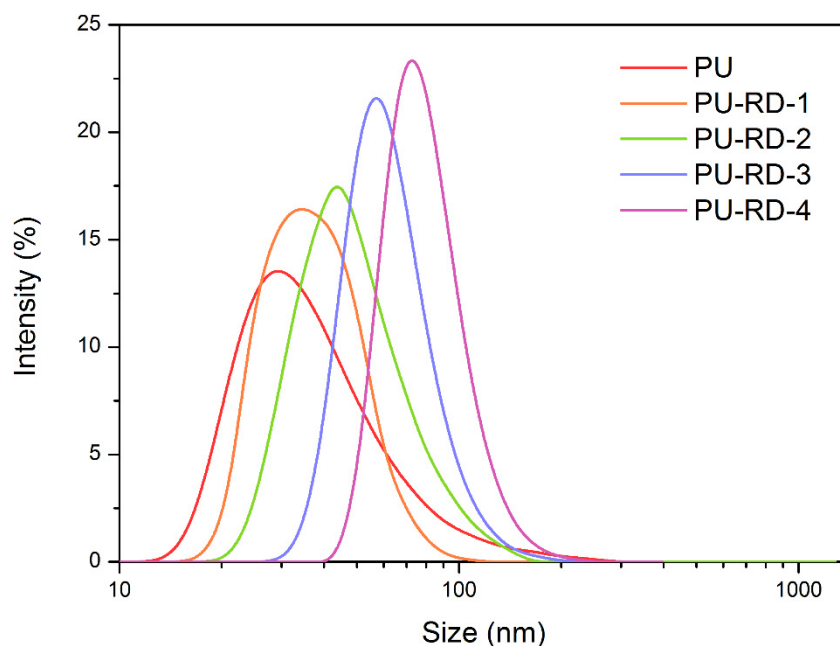


Figure 11. Particle size distribution of PU and PU-RDs emulsions.

Table 3. Average size and particle dispersion index (PDI) of PU and PU-RDs.

	Average Size (nm)	PDI
PU	48.20	0.242
PU-RD-1	53.42	0.222
PU-RD -2	63.83	0.195
PU-RD -3	69.04	0.116
PU-RD -4	78.82	0.104

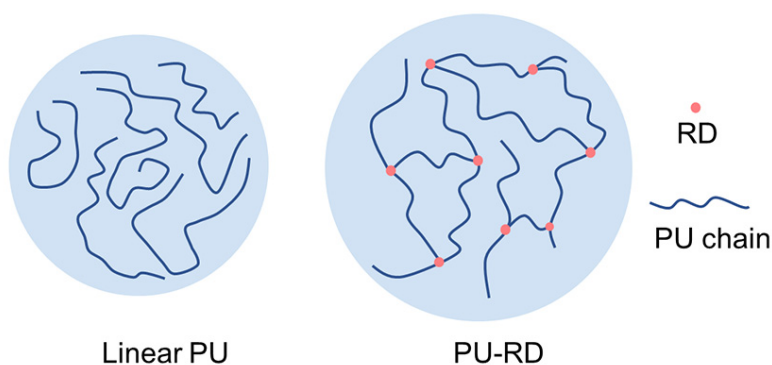


Figure 12. Emulsion particle schematic diagram of PU and PU-RD.

4. Conclusions

In summary, we designed and synthesized fluorescent polyurethanes (PU-RDs) that were covalently cross-linked by rhodamine derivatives (RD). First, RD with three reactive hydrogen was successfully achieved. Afterwards, it was attached into polyurethane chains as cross-linkers. RD and PU-RDs show similar emission shape and the maximum emission wavelength, indicating the fluorescence is still maintained after polymerization. PU-RDs present red in daylight and emit yellow fluorescence under a 365 UV lamp. Due to the cross-linking of polyurethane by $-OH$ and two $-NH-$ of RD, PU-RDs form network structures. The glass-transition temperature, tensile strength, thermal stability, and average size of emulsions increase as the content of RD increase. Because of these unique

properties, as well as the facile and convenient preparation method, this fluorescent polyurethane shows a wide application prospect in coating materials, textiles, anti-fake labels, organic LEDs, and fluorescent probes.

Author Contributions: Conceptualization, S.T. and H.F.; Methodology, S.T.; Investigation, Y.C. and Y.Z.; Writing-Original Draft Preparation, S.T.; Writing-Review & Editing, S.T.; Funding Acquisition, S.T. All authors have read and agreed to the published version of the manuscript.

Funding: This research was funded by Introduce Talent Foundation of Wenzhou University grant number [135010120719].

Acknowledgments: The authors acknowledge financial support from the Introduce Talent Foundation of Wenzhou University (135010120719).

Conflicts of Interest: The authors declare no conflict of interest.

References

1. Cao, H.; Li, B.; Jiang, X.; Zhu, X.; Kong, X.Z. Fluorescent linear polyurea based on toluene diisocyanate: Easy preparation, broad emission and potential applications. *Chem. Eng. J.* **2020**, *399*, 125867. [[CrossRef](#)] [[PubMed](#)]
2. Rene, W.; Lenoble, V.; Chioukh, M.; Branger, C. A turn-on fluorescent ion-imprinted polymer for selective and reliable optosensing of lead in real water samples. *Sens. Actuators B Chem.* **2020**, *319*, 128252. [[CrossRef](#)]
3. Li, D.; Wu, L.; Qu, F.; Ribadeneyra, M.C.; Tu, G.; Gautrot, J.E. Core-independent approach for polymer brush-functionalised nanomaterials with a fluorescent tag for RNA delivery. *Chem. Commun.* **2019**, *55*, 14166–14169. [[CrossRef](#)] [[PubMed](#)]
4. Song, X.; Wang, J.-P.; Song, Y.; Qi, T.; Li, G.L. Bioinspired Healable Mechanochromic Function from Fluorescent Polyurethane Composite Film. *Chemistryopen* **2020**, *9*, 272–276. [[CrossRef](#)]
5. Ghosh, S.; Manna, R.; Dey, S. Polyurethane network using 1-naphthylamine embedded epoxy-based polymer: Ferric ion selective fluorescent probe. *Polym. Bull.* **2019**, *76*, 205–213. [[CrossRef](#)]
6. Liu, H.; Hu, T.; Wang, D.; Shi, J.; Zhang, J.; Wang, J.-X.; Pu, Y.; Chen, J.-F. Preparation of fluorescent waterborne polyurethane nanodispersion by high-gravity miniemulsion polymerization for multifunctional applications. *Chem. Eng. Process. Process. Intensif.* **2019**, *136*, 36–43. [[CrossRef](#)]
7. Li, M.; Qiang, X.; Xu, W.; Zhang, H. Synthesis, characterization and application of AFC-based waterborne polyurethane. *Prog. Org. Coat.* **2015**, *84*, 35–41. [[CrossRef](#)]
8. Lian, F.; Wang, C.; Wu, Q.; Yang, M.; Wang, Z.; Zhang, C. In situ synthesis of stretchable and highly stable multi-color carbon-dots/polyurethane composite films for light-emitting devices. *RSC Adv.* **2020**, *10*, 1281–1286. [[CrossRef](#)]
9. Zhou, J.; Zhang, X.-Y.; Dai, J.; Li, J. Synthesis and Fluorescent Performance of Fluorescein-functionalized Waterborne Polyurethane. *J. Macromol. Sci. Part A* **2012**, *49*, 890–896. [[CrossRef](#)]
10. Akindoyo, J.O.; Beg, D.H.; Ghazali, S.; Islam, M.R.; Jeyaratnam, N.; Yuvaraj, A.R. Polyurethane types, synthesis and applications—A review. *RSC Adv.* **2016**, *6*, 114453–114482. [[CrossRef](#)]
11. Somiseti, V.; Narayan, R.; Raju, K.V.S.N. Multifunctional polyurethane coatings derived from phosphated cardanol and undecylenic acid based polyols. *Prog. Org. Coat.* **2019**, *134*, 91–102. [[CrossRef](#)]
12. Yang, Y.; Cao, X.; Luo, H.; Cai, X. Thermal stability and decomposition behaviors of segmented copolymer poly(urethane-urea-amide). *J. Polym. Res.* **2018**, *25*, 242. [[CrossRef](#)]
13. Gomez, I.J.; Wu, J.; Roper, J.; Beckham, H.; Meredith, J.C.; Roper, I.J.A. High Throughput Screening of Mechanical Properties and Scratch Resistance of Tricomponent Polyurethane Coatings. *ACS Appl. Polym. Mater.* **2019**, *1*, 3064–3073. [[CrossRef](#)]
14. Dong, F.; Maganty, S.; Meschter, S.J.; Cho, J. Effects of curing conditions on structural evolution and mechanical properties of UV-curable polyurethane acrylate coatings. *Prog. Org. Coat. Int. Rev. J.* **2018**, *114*, 58–67. [[CrossRef](#)]
15. Liu, J.; Jiao, X.; Cheng, F.; Fan, Y.; Wu, Y.; Yang, X. Fabrication and performance of UV cured transparent silicone modified polyurethane-acrylate coatings with high hardness, good thermal stability and adhesion. *Prog. Org. Coat.* **2020**, *144*, 105673. [[CrossRef](#)]

16. Zhu, J.; Wu, Z.; Xiong, D.; Pan, L.; Liu, Y.-J. Preparation and properties of a novel low crystallinity cross-linked network waterborne polyurethane for water-based ink. *Prog. Org. Coat.* **2019**, *133*, 161–168. [[CrossRef](#)]
17. Trzebiatowska, P.J.; Echart, A.S.; Calvo-Correas, T.; Eceiza, A.; Datta, J. The changes of crosslink density of polyurethanes synthesised with using recycled component. Chemical structure and mechanical properties investigations. *Prog. Org. Coat.* **2018**, *115*, 41–48. [[CrossRef](#)]
18. Xing, C.; Wang, L.; Xian, L.; Wang, Y.; Zhang, L.; Xi, K.; Zhang, Q.; Jia, X. Enhanced Thermal Ageing Stability of Mechanophore in Polyurethane Network by Introducing Polyhedral Oligomeric Silsesquioxanes (POSS). *Macromol. Chem. Phys.* **2018**, *219*, 1800042. [[CrossRef](#)]
19. Pan, L.; Xiong, Z.; Song, L.; Ban, J.-F.; Lu, S. Synthesis and characterization of sisal fibre polyurethane network cross-linked with triple-shape memory properties. *New J. Chem.* **2018**, *42*, 7130–7137. [[CrossRef](#)]
20. Qian, Y.; An, X.; Huang, X.; Pan, X.; Zhu, J.; Zhu, X. Recyclable Self-Healing Polyurethane Cross-Linked by Alkyl Diselenide with Enhanced Mechanical Properties. *Polymers* **2019**, *11*, 773. [[CrossRef](#)]
21. Hermida-Merino, D.; O'Driscoll, B.; Hart, L.R.; Harris, P.J.F.; Colquhoun, H.M.; Slark, A.T.; Priscariu, C.; Hamley, I.W.; Hayes, W. Enhancement of microphase ordering and mechanical properties of supramolecular hydrogen-bonded polyurethane networks. *Polym. Chem.* **2018**, *9*, 3406–3414. [[CrossRef](#)]
22. Arévalo-Alquichire, S.; Morales-Gonzalez, M.; Navas-Gómez, K.; Díaz, L.E.; Gómez-Tejedor, J.; Serrano, M.-A.; Valero, M.F. Influence of Polyol/Crosslinker Blend Composition on Phase Separation and Thermo-Mechanical Properties of Polyurethane Thin Films. *Polymers* **2020**, *12*, 666. [[CrossRef](#)] [[PubMed](#)]
23. Yi, J.; Huang, C.; Zhuang, H.; Gong, H.; Zhang, C.; Ren, R.; Ma, Y. Degradable polyurethane based on star-shaped polyester polyols (trimethylolpropane and E-caprolactone) for marine antifouling. *Prog. Org. Coat.* **2015**, *87*, 161–170. [[CrossRef](#)]
24. Chattopadhyay, D.K.; Sreedhar, B.; Raju, K.V.S.N. Thermal stability of chemically crosslinked moisture-cured polyurethane coatings. *J. Appl. Polym. Sci.* **2010**, *95*, 1509–1518. [[CrossRef](#)]
25. Yarmohammadi, M.; Komeili, S.; Shahidzadeh, M. Studying Crosslinker Chemical Structure Effect on the Tuning Properties of HTPB-Based Polyurethane. *Propellants Explos. Pyrotech.* **2018**, *43*, 156–161. [[CrossRef](#)]
26. Diao, Q.; Guo, H.; Yang, Z.; Luo, W.; Li, T.; Hou, D. A rhodamine-6G-based “turn-on” fluorescent probe for selective detection of Fe³⁺ in living cells. *Anal. Methods* **2019**, *11*, 794–799. [[CrossRef](#)]
27. Berube, M.-A.; Schorr, D.; Ball, R.J.; Landry, V.; Blanchet, P. Determination of In Situ Esterification Parameters of Citric Acid-Glycerol Based Polymers for Wood Impregnation. *J. Polym. Environ.* **2018**, *26*, 970–979. [[CrossRef](#)]
28. Marques, N.D.N.; Balaban, R.D.C.; Halila, S.; Borsali, R. Synthesis and characterization of carboxymethylcellulose grafted with thermoresponsive side chains of high LCST: The high temperature and high salinity self-assembly dependence. *Carbohydr. Polym.* **2018**, *184*, 108–117. [[CrossRef](#)]
29. Datta, J.; Głowińska, E. Effect of hydroxylated soybean oil and bio-based propanediol on the structure and thermal properties of synthesized bio-polyurethanes. *Ind. Crop. Prod.* **2014**, *61*, 84–91. [[CrossRef](#)]
30. Hu, X.; Liu, X.; Liu, M.; Li, G.; Cheng, C. A photochromic waterborne polyurethane-based dye with chemically fixed azobenzene groups. *Polym. Bull.* **2019**, *76*, 3437–3450. [[CrossRef](#)]
31. Fujii, K.; Iyi, N.; Sasai, R.; Hayashi, S. Preparation of a Novel Luminous Heterogeneous System: Rhodamine/Coumarin/Phyllosilicate Hybrid and Blue Shift in Fluorescence Emission. *Chem. Mater.* **2008**, *20*, 2994–3002. [[CrossRef](#)]
32. Yang, Z.; Wicks, D.A.; Yuan, J.; Pu, H.; Liu, Y. Newly UV-curable polyurethane coatings prepared by multifunctional thiol- and ene-terminated polyurethane aqueous dispersions: Photopolymerization properties. *Polymers* **2010**, *51*, 1572–1577. [[CrossRef](#)]
33. Crawford, D.M.; Escarsega, J.A. Dynamic mechanical analysis of novel polyurethane coating for military applications. *Thermochim. Acta* **2000**, *357*, 161–168. [[CrossRef](#)]
34. Campanella, A.; Bonnaillie, L.M.; Wool, R.P. Polyurethane foams from soyoil-based polyols. *J. Appl. Polym. Sci.* **2009**, *112*, 2567–2578. [[CrossRef](#)]
35. Chiou, B.-S.; Schoen, P.E. Effects of crosslinking on thermal and mechanical properties of polyurethanes. *J. Appl. Polym. Sci.* **2002**, *83*, 212–223. [[CrossRef](#)]
36. Koczyńska, P.; Datta, J.; Trzebiatowska, P.J. Single-phase product obtained via crude glycerine depolymerisation of polyurethane elastomer: Structure characterisation and rheological behaviour. *Polym. Int.* **2016**, *65*, 946–954. [[CrossRef](#)]

37. Camino, G.; Lomakin, S.M.; Lazzari, M. Polydimethylsiloxane thermal degradation Part 1. Kinetic aspects. *Polymer* **2001**, *42*, 2395–2402. [[CrossRef](#)]
38. Ma, M.; Sun, G. Antimicrobial cationic dyes: Part 2—Thermal and hydrolytic stability. *Dyes Pigment* **2004**, *63*, 39–49. [[CrossRef](#)]
39. Mao, H.; Wang, C.; Wang, Y. Synthesis of polymeric dyes based on waterborne polyurethane for improved color stability. *New J. Chem.* **2015**, *39*, 3543–3550. [[CrossRef](#)]
40. Deshpande, G.; Rezac, M.E. The effect of phenyl content on the degradation of poly(dimethyl diphenyl) siloxane copolymers. *Polym. Degrad. Stab.* **2001**, *74*, 363–370. [[CrossRef](#)]
41. Wang, L.; Shen, Y.; Lai, X.; Li, Z. Effect of nanosilica content on properties of polyurethane/silica hybrid emulsion and its films. *J. Appl. Polym. Sci.* **2010**, *119*, 3521–3530. [[CrossRef](#)]



© 2020 by the authors. Licensee MDPI, Basel, Switzerland. This article is an open access article distributed under the terms and conditions of the Creative Commons Attribution (CC BY) license (<http://creativecommons.org/licenses/by/4.0/>).